SUMO-assisted expression of a soluble and functional Venus flytrap domain of the human sweet taste receptor TAS1R2 in Escherichia coli

Christine Belloir, Adeline Karolkowski, Lucie Moitrier, Loïc Briand

Protein Expression and Purification 242 (2026) 106936

Contents lists available at ScienceDirect

Protein Expression and Purification

journal homepage: www.elsevier.com/locate/yprep

Research Article

SUMO-assisted expression of a soluble and functional Venus flytrap domain of the human sweet taste receptor TAS1R2 in *Escherichia coli*

Christine Belloir [1], Adeline Karolkowski [1], Lucie Moitrier, Loïc Briand [*]

Université Bourgogne Europe, Institut Agro, CNRS, INRAE, UMR CSGA, Dijon, 21000, France

ARTICLE INFO

Keywords:
Taste receptor
Sugar
Sweetener
GPCR
SUMO
Bacterial expression

ABSTRACT

The heterodimeric human sweet taste receptor TAS1R2/TAS1R3 is a class C G-protein-coupled receptor responsible for detecting a wide range of sweet-tasting compounds. The Venus flytrap domain of hTAS1R2 (hTAS1R2-VFT) constitutes the main binding site for natural sugars and some noncaloric sweeteners, including sucralose, neotame, and acesulfame-K. However, its biophysical characterization has been limited by difficulties in producing soluble and functional protein, with most strategies relying on refolding from inclusions bodies. In this study, we report the successful expression of soluble, folded, and functional hTAS1R2-VFT using *Escherichia coli* and a N-terminal small ubiquitin-like modifier (SUMO) fusion protein, avoiding protein refolding from inclusion bodies. A two-step purification process (immobilized metal ion affinity chromatography followed by preparative gel filtration) yielded approximately 0.42 mg of pure protein per liter of culture. Circular dichroism spectroscopy and size-exclusion chromatography coupled with multiangle static light scattering analysis confirmed proper folding and monomeric behavior of SUMO-hTAS1R2-VFT. Functional characterization using intrinsic tryptophan fluorescence revealed that SUMO-hTAS1R2-VFT bound sweet-tasting compounds with affinities consistent with their physiological relevance. Neotame exhibited the highest affinity ($K_d \approx 2$ μM), followed by acesulfame-K ($K_d \approx 116$ μM) and sucralose ($K_d \approx 282$ μM), while sucrose showed weak binding in the millimolar range. These affinities were in agreement with sweetness potency and comparable to those reported for the full-length TAS1R2 subunit. This work provides the first demonstration of soluble expression of functional hTAS1R2-VFT in bacteria, by adding a solubility tag, offering a robust and scalable platform for studying sweetener-receptor interactions and facilitating the rational design of novel sweeteners.

1. Introduction

Humans can detect and discriminate 5 basic tastes, namely, sweet, umami, bitter, salty, and sour [1]. Sweet taste plays a key role in the detection of carbohydrate-rich foods, which represent a primary source of readily available energy. Many compounds, in addition to natural sugars (glucose, fructose, and sucrose), and polyols are perceived as sweet, including natural sweeteners (steviosides, hernandulcin, glycyrrhizin and mogrosides), sweet amino acids, artificial sweeteners (acesulfame-K (Ace-K), saccharin, cyclamate, and neotame) and semisynthetic sweeteners (sucralose, neohesperidin dihydrochalcone (NHDC) and perillartine) [2,3]. In addition plant sweet-tasting proteins, including brazzein, pentadin, monellin, thaumatin, and neoculin, also elicit a sweet taste [2,3]. All these diverse types of sweet-tasting compounds are recognized by a single heterodimeric class C G-protein-coupled receptor (GPCR) located in taste buds. This receptor is composed of the obligatory assembly of 2 subunits, namely TAS1R2/-TAS1R3 [4,5]. These 2 subunits share a similar structure made up of a large extracellular domain consisting of a Venus flytrap domain (VFT) and a cysteine-rich domain (CRD) linked to the 7-helix transmembrane domain (7TM). The sweet taste receptor exhibits low binding affinities for natural sugars (in the millimolar range), and higher affinities with artificial sweeteners, which are in agreement with their sweetness potency [6–8]. TAS1R2/TAS1R3 receptor exhibits multiple binding sites for sweet-tasting compounds, which explains the chemical diversity of sweet-tasting compounds [9–11] and the sweet taste synergies observed with sweetener blends [7]. It has been shown that human TAS1R2-VFT (hTAS1R2-VFT) contains the main ligand-binding site of the sweet taste

* Corresponding author.
E-mail addresses: christine.belloir@inrae.fr (C. Belloir), adeline.karolkowski@inrae.fr (A. Karolkowski), lucie.moitrier@inrae.fr (L. Moitrier), loic.briand@inrae.fr (L. Briand).
[1] C.B. and A.K. contributed equally to this work and should be considered as co-first authors.

https://doi.org/10.1016/j.pep.2026.106936
Received 4 March 2026; Received in revised form 22 April 2026; Accepted 26 April 2026
Available online 1 May 2026

receptor, notably for natural sugars and most sweeteners (sucralose, aspartame, neotame, Ace-K, saccharin and steviosides), whereas hTAS1R3-VFT has been shown to interact with sucrose, glucose, and sucralose [12–18]. Notably, these 3 compounds bind to hTAS1R2- and hTAS1R3-VFTs with distinct binding affinities and conformational changes [12]. hTAS1R2- and hTAS1R3-7TMs contain binding sites for perillartine and, cyclamate and NHDC, respectively [9,19–21]. Molecular modeling and human/rodent chimeras have revealed that the 2 sweet-tasting proteins, brazzein and thaumatin, interact with the CRD of hTAS1R2/hTAS1R3 [14,22,23]. Recently, cry-electron microscopy (cryo-EM) studies conducted by three independent research groups revealed the overall organization of the full-length hTAS1R2/hTAS1R3 receptor and provided structural insights into ligand recognition and the mechanism of receptor activation. Notably, natural sugars were consistently observed to bind within the VFT of hTAS1R2, whereas no sugar-binding site was identified in hTAS1R3-VFT, confirming the predominant role of hTAS1R2 in sugar recognition [24–26].

One of the main limitations in studying the molecular mechanisms of ligand binding is the difficulty in producing sufficient amounts of soluble and functional sweet taste receptor complexes suitable for biochemical and biophysical analyses [15,27]. To overcome these limitations, several recombinant expression strategies have been developed (Table 1). Early efforts to express isolated VFT domains in *Escherichia coli* (*E. coli*) aimed at improving solubility through fusion strategies. Notably, the VFT domains of mouse TAS1R2 and TAS1R3 were expressed as N-terminal fusions with maltose-binding protein (MBP) or with a chitin-binding domain (CBD), which increased their solubility and enabled functional characterization [12,28]. These recombinant proteins, in the absence of eukaryotic modification, were able to bind sweet-tasting compounds, although with distinct affinities and conformational changes [12,28]. Subsequent studies focused on hTAS1R domains, including hTAS1R3-VFT [16,29] and later hTAS1R2-VFT, which were predominantly expressed in *E. coli* as inclusion bodies (IBs) [15]. Following purification under denaturing conditions, proteins were refolded *in vitro* to recover their functional conformations. This strategy enabled the production of substantial amounts of recombinant protein (approximately 110 mg/L of bacterial culture for hTAS1R3-VFT and up to 200 mg/L for hTAS1R2-VFT as IBs), and ligand binding was assessed using biophysical approaches such as intrinsic tryptophan fluorescence, yielding dissociation constants consistent with physiological detection ranges [15,16,29]. For example, hTAS1R3-VFT is capable of binding sucralose with an affinity in the millimolar range [16,29]. More recently, hTAS1R3-7TM encompassing the CRD was expressed in bacteria as IBs, purified by immobilized metal affinity chromatography (IMAC) and refolded. K_d values measured using intrinsic fluorescence revealed binding of hTAS1R3-7TM with sucrose, sucralose, and brazzein [30]. Similarly, we expressed in bacteria as IBs and refolded to yield functional proteins, human and cat TAS1R1-VFTs and hTAS1R3-VFT, which are components of the umami taste receptor (TAS1R1/TAS1R3) [31,32]. Although IB-based expression allows for high protein yields, it requires labor-intensive and time-consuming refolding steps, involving large buffer volumes and costly low molecular additives and detergents. In addition, the refolding strategy from IBs may result in variable recovery and reduced functional yields [33]. The use of small ubiquitin-like modifier (SUMO) fusion protein has emerged as an alternative strategy to enhance protein solubility and folding in bacterial systems [34,35]. Nevertheless, previous applications of SUMO tag to enhance the overall stability and activity of TAS1R2-VFT did not eliminate the need for IB isolation and refolding. In addition, this expression strategy required additional proteolytic cleavage steps, leading to a modest final yield (5-10 mg/L) [27]. Nevertheless, biophysical analyses demonstrated that refolded hTAS1R2-VFT SUMO fusion protein bound different sweet-tasting compounds (sucrose, sucralose, neotame, and Ace-K) with K_d values in the micromolar range (40-100 μM) [27].

In this context, the present study introduces a distinct approach based on SUMO-assisted expression that enables the direct production of soluble hTAS1R2-VFT in *E. coli*, bypassing denaturation and refolding steps entirely. Compared with previous strategies, this method simplifies the production workflow, reduces detergent use, and improves reproducibility while yielding a properly folded and functional protein. A two-step purification method, including IMAC and preparative gel filtration, was employed to purify the detergent-solubilized SUMO-hTAS1R2-VFT protein present in the soluble fraction. Then, the soluble and purified SUMO-hTAS1R2-VFT was structurally and functionally characterized using several biophysical methods, including circular dichroism (CD) spectroscopy, size exclusion chromatography coupled with multiangle static light scattering (SEC-MALS) and intrinsic tryptophan fluorescence.

2. Materials and methods

2.1. Sweeteners

Sucralose, neotame, Ace-K, and sucrose with a purity ≥ 85% were obtained from Sigma-Aldrich (Saint-Quentin Fallavier, France) and stored according to the manufacturer's instructions.

2.2. Construction of the SUMO-hTAS1R2-VFT expression vector

The cDNA sequence encoding the hTAS1R2-VFT (accession number NM_152232.5), lacking a putative signal peptide and the CRD, was cloned and inserted into a pET-SUMO expression vector (Eurogentec,

Table 1
Comparison of expression strategies for TAS1R subunits production.

Proteins of interest	Expression system	Strategy	Yield	Functional outcomes	References
mTAS1R2-VFT, mTAS1R3-VFT	*E. coli*	N-terminal MBP/CBD fusion	-	- Soluble - Functional - Ligand binding with distinct affinities (glucose, sucrose, sucralose)	[12,28]
hTAS1R3-VFT	*E. coli*	IBs, refolded	~110 mg/L	- Functional after refolding - Ligand binding with distinct affinity (sucralose)	[16,29]
hTAS1R2-VFT	*E. coli*	IBs, refolded	Up to 200 mg/L	- Functional after refolding - Ligand binding with distinct affinities (lactose, glucose, fructose, sucrose, acesulfame-K, aspartame, saccharin, sucralose, alitame, neotame)	[15]
hTAS1R3-7TM	*E. coli*	IBs, refolded	-	- Functional after refolding - Ligand binding with distinct affinities (sucrose, sucralose, brazzein)	[30]
cTAS1R1-VFT, hTAS1R1-VFT, hTAS1R3-VFT	*E. coli*	IBs, refolded	-	- Functional after refolding - Ligand binding (inosine-5′-monophosphate, several amino acids)	[31,32]
mTAS1R2-VFT, hTAS1R2-VFT	*E. coli*	N-terminal SUMO fusion, IBs, refolded, SUMO cleavage site	5-10 mg/L	- Functional after refolding and SUMO removing - Ligand binding (sucrose, sucralose, neotame, acesulfame-K)	[27]

MBP: maltose-binding protein; CBD: chitin-binding domain; IB: inclusion body.

Seraing, Belgium) and expressed in *E. coli* BL21(DE3) cells. The resulting expression plasmid, pET-SUMO-hTAS1R2-VFT, encoded a SUMO fusion protein with an N-terminal 6x-His tag (which could be cleaved by SUMO protease), followed by hTAS1R2-VFT (Ala22-Ser493) and C-terminal 6x-His tag (Fig. 1, Table S1).

2.3. Expression and production of soluble functional SUMO-hTAS1R2-VFT

To produce SUMO-hTAS1R2-VFT, *E. coli* BL21 (DE3) cells containing the pET-SUMO-hTAS1R3-VFT plasmid were grown in 2 L Luria Bertani (LB) medium supplemented with kanamycin (50 μg/mL) at 37 °C to reach an optical density of 0.4-0.6 at 600 nm, as recommended by the manufacturer instructions. The induction of protein expression was carried out by the addition of 0.1 mM isopropyl-β-D-thiogalactoside (IPTG) at 20 °C for 20 h. Then, the cells were collected by centrifugation (6,000 *g* for 20 min at 4 °C).

The cell pellet from 2 L of culture was resuspended in 20 mL of ice-cold lysis buffer (50 mM potassium phosphate (pH 7.8), 400 mM NaCl, 100 mM KCl, 10% glycerol, 0.5% Triton X-100, 0.1 mM DDM (N-dodecyl β-D-maltoside) and 10 mM imidazole). After resuspension, 1 protease inhibitor cocktail tablet was added (cOmplete™ Mini, Roche Diagnostics, Mannheim, Germany), and the suspension was disrupted by sonication (Vibra Cell, Sonics & Materials, Newtown, CT, USA) twice for 2 min. After centrifugation (24,000 *g* for 30 min, 4 °C), the supernatant containing the soluble fraction was filtered through a 0.22 μm filter. The pellet was also retained for analysis.

A two-step purification method, including IMAC and preparative gel filtration, was employed to purify the detergent-solubilized SUMO-hTAS1R2-VFT protein from the soluble fraction. First, the soluble fraction was applied to a 1 mL His-Trap™ HP column (GE Healthcare, Vélizy-Villacoublay, France) in a closed circuit for 24 h, enabling the isolation of soluble SUMO-hTAS1R2-VFT protein. Before the sample was added, the column was washed at a gradient of 0.5 mL/min with 4 mL ultrapure water, 4 mL buffer A (50 mM potassium phosphate (pH 7.8), 150 mM NaCl, 0.1 mM DDM, 20 mM imidazole), 4 mL buffer B (50 mM potassium phosphate (pH 7.8), 150 mM NaCl, 0.1 mM DDM, 500 mM imidazole) and 2 x 2 mL buffer A. Second, the IMAC fractions containing SUMO-hTAS1R2-VFT were pooled and concentrated to 500 μL using a 30-kDa MWCO filter column (Vivaspin, Sartorius, Aubagne, France). The samples were then subjected to preparative gel filtration chromatography (Superdex® 200 Increase 30/300 GL column, Sigma-Aldrich) on an Äkta Pure FPLC system (GE Healthcare). The column was equilibrated with 2 column volumes of wash buffer (50 mM Tris-HCl (pH 8.0), 150 mM NaCl, 0.1 mM DDM, and 1 mM DTT (dithiothreitol)) before the purified SUMO-hTAS1R2-VFT sample was applied. After loading, the column was washed with wash buffer at 0.5 mL/min, and the column flow through was monitored by measuring the UV absorbance at 280 nm. The same IMAC fraction was injected 3 to 4 times. Aliquots of samples collected during the purification process were pooled and analyzed by sodium dodecyl sulfate-polyacrylamide gel electrophoresis (SDS-PAGE) and Western blotting, and their absorbance at 280 nm was measured to determine the protein concentration, as previously described [15].

Fig. 1. Construction of SUMO-hTAS1R2-VFT expression vector. hTAS1R2-VFT, lacking a putative signal peptide and the CRD, was cloned and inserted into a pET-SUMO expression vector and expressed in *E. coli* BL21(DE3) cells. Two 6x-His tags were added at the N- and C-terminal positions.

2.4. Circular Dichroism (CD) spectroscopy

CD spectroscopy analyses were carried out on SUMO-hTASR2-VFT as described previously [15,17,32]. CD spectra were recorded using a JASCO J-815 spectropolarimeter (Jasco, Tokyo, Japan) equipped with a Peltier temperature controller. Measurements were recorded at 20 °C using a quartz cuvette with a 0.01 cm path length, over the wavelength range of 190-260 nm, at 0.5 nm intervals and a scan speed of 50 nm/min. Data were averaged from 10 accumulated scans. Buffer contributions were subtracted, and the data were converted to mean residue ellipticity (deg·cm^2·dmol^{-1}). Secondary structure proportions were calculated using the Beta Structure Selection (BeStSel) webserver (https://bestsel.elte.hu/, accessed on 26 March 2026) (ELTE Eötvös Loránd University, Budapest, Hungary) [36].

2.5. Size Exclusion Chromatography with Multiangle Static Light Scattering (SEC-MALS)

The oligomeric state of the purified SUMO-hTAS1R2-VFT protein was assessed, as described previously [31], using a Jasco PU-2080 Plus HPLC system (Jasco, Cremella, Italy), consisting of a pump, a vacuum degasser and an autosampler, and a Silica Gel KW803 column (Shodex, Munich, Germany) coupled to a triple-angle light-scattering detector (Mini-DAWN™ TREOS, Wyatt Technology, Toulouse, France), a differential refractometer (Ri-4030 Refractive Index Detector, Jasco) and a UV detector (UV-4070 UV/Vis Detector, Jasco) at 280 nm. The molecular weight was determined using ASTRA VI software (version 6.1; Wyatt Technology) with a dn/dc value of 0.185 mL/g for analysis. After equilibration with wash buffer, an aliquot of 100 μL of the fraction at a concentration of 0.2 mg/mL was injected at a flow rate of 0.5 mL/min.

2.6. Intrinsic tryptophan fluorescence

As described previously [15,17,32], measurements were performed at 20 °C using a Cary Eclipse spectrofluorometer (Agilent Technologies, Santa Clara, CA, USA) equipped with a Peltier temperature control unit, with emission and excitation bandwidths set to 5 nm. Ligand binding assays with 0.15 mg/mL SUMO-hTAS1R2-VFT were conducted in buffer containing 50 mM Tris-HCl (pH 8.0), 150 mM NaCl, 0.1 mM DDM, and 1 mM DTT. The intrinsic fluorescence of SUMO-hTAS1R2-VFT was measured at an excitation wavelength of 295 nm, with emission spectra recorded between 320 and 380 nm. Fluorescence emission was monitored at 350 nm in the presence and absence of sweet-tasting compounds. The compounds were freshly prepared in 50 mM Tris-HCl (pH 8.0). Fluorescence data were corrected for bleaching, dilution, and nonspecific buffer quenching. The dissociation constants (K_d) were calculated from a plot of the ratio between the fluorescence intensity variation and the maximum fluorescence intensity variation ($\Delta F/\Delta F_{max}$) versus the concentration of the total ligand. Assuming that the binding of SUMO-hTAS1R2-VFT to sweet-tasting compounds follows a one-site binding model, K_d values were calculated using standard nonlinear regression with SigmaPlot 12.5 software (Systat Software, Inc., San Jose, CA, USA).

Statistical data analysis was performed on maximal fluorescence intensity of SUMO-hTAS1R2-VFT following titration with buffer or different ligands (sucralose, neotame, Ace-K, and sucrose), using XLSTAT 2023 (Lumivero, Denver, CO, USA).

3. Results

3.1. Expression and purification of SUMO-hTAS1R2-VFT

To produce functional recombinant hTAS1R2-VFT, we expressed SUMO-hTAS1R2-VFT using an *E. coli* prokaryotic expression system. SDS-PAGE and Western blot analysis revealed a band migrating at a molecular weight of approximately 75 kDa (Fig. 2A–B), in agreement

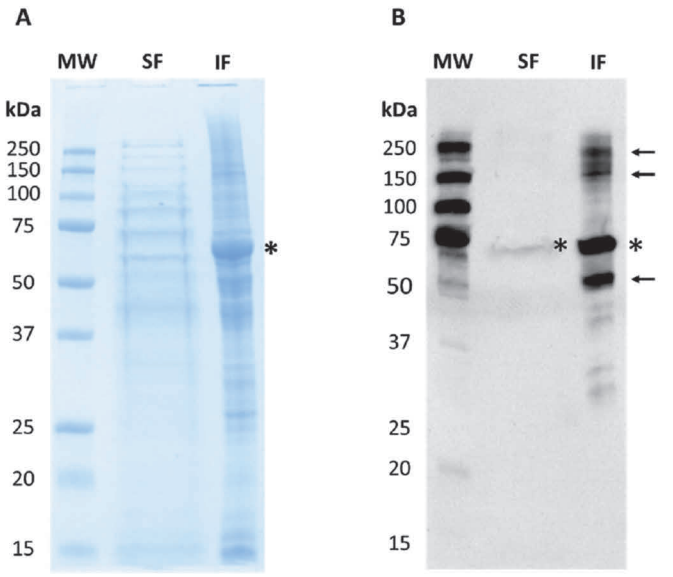

Fig. 2. SDS-PAGE (A) and Western-blot (B) analysis of SUMO-hTAS1R2-VFT. (A) Proteins from the soluble fraction (SF) and proteins from the insoluble fraction (IF, known as inclusion bodies), were separated on 10% acrylamide gels and stained with Coomassie blue. (B) Western blot analysis using a mouse anti-His primary antibody and goat anti-mouse horseradish peroxidase-conjugated secondary antibody revealed the presence of SUMO-hTAS1R2-VFT in both SF and IF. The position of SUMO-hTAS1R2-VFT is indicated by an asterisk in both analyses. The arrows indicate multimeric forms and proteolytic fragment of SUMO-hTAS1R2-VFT. MW: molecular weight markers. (For interpretation of the references to color in this figure legend, the reader is referred to the Web version of this article.)

with the theoretical molecular mass value (73.8 kDa) calculated from the protein sequence, confirming that SUMO-hTAS1R2-VFT was expressed after IPTG induction. SUMO-hTAS1R2-VFT was mainly detected in the insoluble fraction as insoluble aggregates. However, a small amount of soluble SUMO-hTAS1R2-VFT was observed in the soluble fraction.

The soluble fraction containing SUMO-hTAS1R2-VFT was then purified using IMAC. The chromatogram revealed 2 distinct peaks eluted at approximatively 6 and 8 mL, respectively (Fig. 3A). Fractions 7 to 16 were analyzed by SDS-PAGE, which revealed that SUMO-hTAS1R2-VFT was present in most fractions, resulting in a band migrating to a molecular weight of approximately 75 kDa (Fig. 3B). Fractions 11 to 15, corresponding to peak 2 and showing stronger bands, were pooled together. The protein yield was approximately 3.1 mg of SUMO-hTAS1R2-VFT per liter of bacterial culture.

To further purify the soluble protein, we performed preparative gel filtration chromatography. Chromatographic analysis revealed several peaks, notably, the third peak eluted at 13.5 mL and corresponded to fraction 19 (Fig. 4A). SDS-PAGE and Western blot analysis (Fig. 4B and C) revealed that purified SUMO-hTAS1R2-VFT protein, which corresponded to the band migrating at approximately 75 kDa, was mainly detected in fractions 18 to 20. These data suggested that SUMO-hTAS1R2-VFT behaved as a monomer. While very faint bands around ~80 kDa and ~30 kDa were visible, they represented minor impurities which did not affect the overall purity of the interested protein (≥ 90%) in fraction 19. Finally, from 3.1 mg of IMAC-purified protein, we obtained approximately 0.42 mg of soluble and purified SUMO-hTAS1R2-VFT.

3.2. Characterization of SUMO-hTAS1R2-VFT

To confirm the correct folding of SUMO-hTAS1R2-VFT, far-UV CD spectroscopy was carried out. The CD spectrum was characterized by a high content of α-helix-structures, with a maximal positive peak at 193 nm and 2 minimal negative peaks at approximatively 208 and 220 nm (Fig. 5A). This spectrum was similar to that obtained for human and mouse TAS1R2-VFT, mouse MBP-TAS1R2-VFT, human and mouse TAS1R3-VFT, and mouse MBP-TAS1R3-VFT [12,15,16,27,29,31]. SUMO-hTAS1R2-VFT was composed of approximately 25.5% α-helices and 16.3% β-sheets. SEC-MALS analysis allowed us to determine the oligomerization state of SUMO-hTAS1R2-VFT purified from fraction 19 obtained during preparative gel filtration. The results revealed the presence of SUMO-hTAS1R2-VFT in a homogenous form, with an average molecular weight of approximatively 70 kDa (Fig. 5B). The theoretical mass of SUMO-hTAS1R2-VFT was 73.8 kDa suggested that the purified protein appeared mainly as a monomer.

3.3. Ligand binding properties of SUMO-hTAS1R2-VFT

The intrinsic tryptophan fluorescence spectra of purified SUMO-hTAS1R2-VFT were measured in presence of increasing concentrations of sweet-tasting compounds, allowing to determine the changing environment around tryptophan residues as an indicator of ligand binding. The protein sequence contains 10 tryptophan (W) residues located at positions W203, W205, W298, W304, W341, W418, W425, W453, W455, and W483, which were distributed within the VFT domain and may differentially contribute to the fluorescence signal depending on

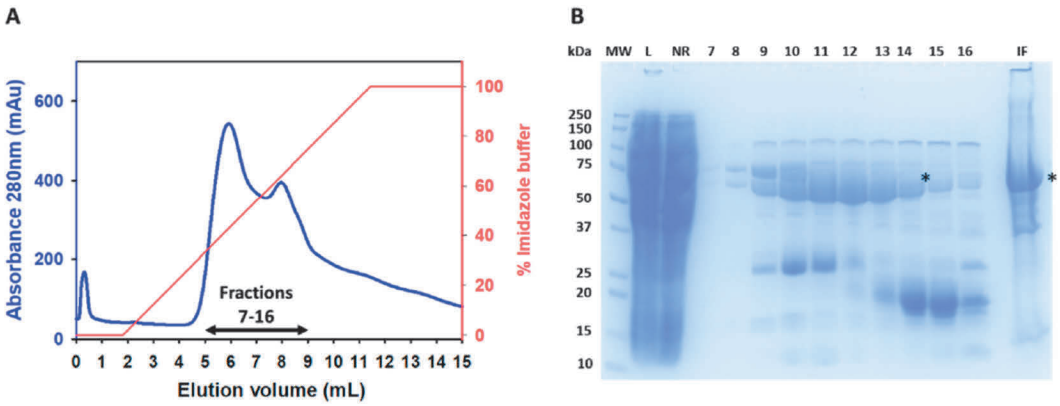

Fig. 3. IMAC purification (A) and SDS-PAGE analysis (B) of SUMO-hTAS1R2-VFT. (A) The last 2 peaks eluted at approximately 6 and 8 mL, respectively, and corresponded to fractions 7-16 were analyzed by (B) SDS-PAGE followed by staining with Coomassie blue. IF was loaded on SDS-PAGE as a control. Fractions 11-15 contained mainly SUMO-hTAS1R2-VFT, were used for subsequent measurements. The position of SUMO-hTAS1R2-VFT is indicated by an asterisk in the SDS-PAGE analysis. MW: molecular weight markers; L: loaded samples; NR: not retained; IF: insoluble fraction (containing inclusion bodies). (For interpretation of the references to color in this figure legend, the reader is referred to the Web version of this article.)

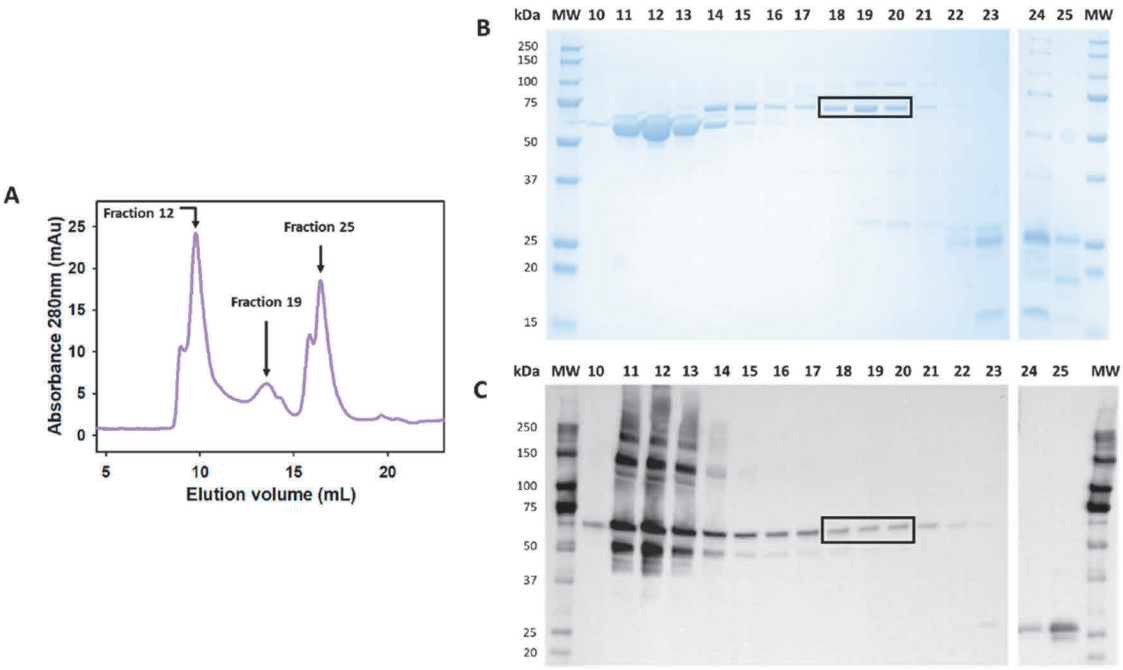

Fig. 4. Preparative gel filtration chromatography (A), SDS-PAGE (B) followed by staining with Coomassie blue and Western blot (C) analysis of SUMO-hTAS1R2-VFT using a mouse anti-His primary antibody and goat anti-mouse horseradish peroxidase-conjugated secondary antibody. (A) Several peaks were present, including peak 3 (elution volume at 13.5 mL), and corresponded to fraction 19. (B-C) Fractions 18-20 contained mainly SUMO-hTAS1R2-VFT, indicated by a black frame. M: molecular weight markers. (For interpretation of the references to color in this figure legend, the reader is referred to the Web version of this article.)

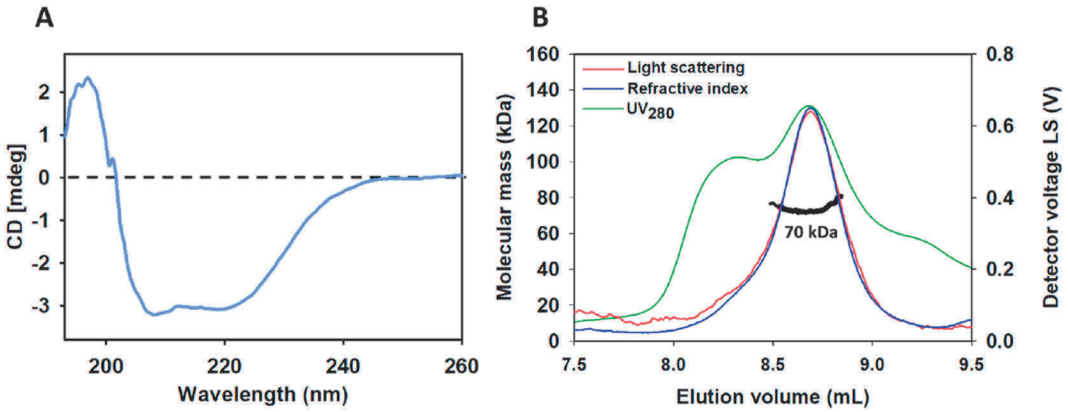

Fig. 5. Secondary structure (A) analysis using CD spectroscopy and oligomeric state (B) analysis using SEC-MALS of purified SUMO-hTAS1R2-VFT. (A) Far-UV CD spectrum of SUMO-hTAS1R2-VFT (N = 1) revealed a high content of α-helical secondary structures (25.5%). Protein concentration was 0.2 mg/mL, and light path was 0.01 cm. (B) For SEC-MALS analysis, purified SUMO-hTAS1R2-VFT was injected into a Silica Gel KW803 column (Shodex) and eluted (50 mM Tris-HCl (pH 7.5), 150 mM NaCl, 1 mM DTT and 0.1 mM DDM). The chromatogram shows the calculated molecular mass (bold black curve), refractive index (blue curve), light scattering (red curve) and UV at 280 nm (green curve). SUMO-hTAS1R2-VFT had a fitted molecular mass of approximatively 70 kDa (with a theoretical monomer molecular mass value of 73.8 kDa). (For interpretation of the references to color in this figure legend, the reader is referred to the Web version of this article.)

their local environment (Table S1). This method has been previously used to characterize protein-ligand binding interactions with mouse, cat, and human TAS1R-VFTs [12,15,16,32]. The addition of increasing concentrations of sucralose (0-3438 μM) modified the shape of the spectrum. The emission maximum shifted from 335 nm (0-58 μM) to 355 nm (738-3438 μM), accompanied by a progressive increase in intrinsic fluorescence intensity (Fig. 6A). An increase in fluorescence was detectable at 58 μM sucralose and reached a plateau at 1044 μM, with no further significant increase observed at 2653 and 3438 μM, indicating a saturable binding process. In contrast, increasing sucrose concentrations (0-700 mM) produced only a slight increase in fluorescence intensity, from 381 a.u. (0-202 mM) to 400 a.u. (513-700 mM), without affecting the spectral shape or emission maximum (Fig. 6B). No clear saturation behavior was observed within the tested concentration range. This limited impact on tryptophan fluorescence suggested that sucrose binding slightly changed the local environment of these residues. One possible explanation was that sucrose induced a different protein conformation compared to sucralose, in which the tryptophan residues were only weakly affected or not directly involved in the binding site. Alternatively, sucrose may interact with regions of the protein that were distant from the tryptophan residues, resulting in minimal fluorescence changes despite potential binding. Interestingly, the addition of sucralose and sucrose produced distinct effects on tryptophan residues, leading to different spectra and suggesting distinct ligand-specific conformational changes. Halogenated compounds, such as sucralose, are known to strongly quench tryptophanyl fluorescence.

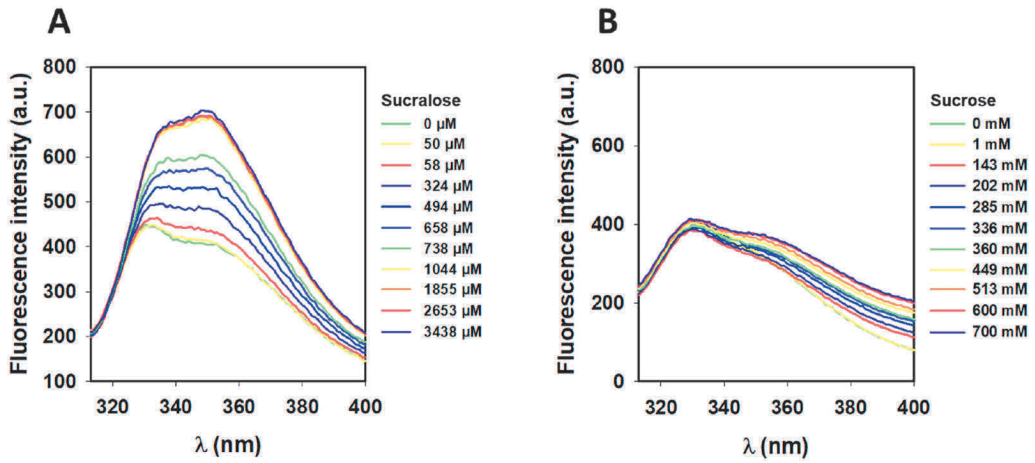

Fig. 6. Intrinsic fluorescence emission spectra of 0.15 mg/mL purified SUMO-hTAS1R2-VFT in the presence of increasing concentrations of (A) sucralose (0-3438 µM) and (B) sucrose (0-700 mM). (For interpretation of the references to color in this figure legend, the reader is referred to the Web version of this article.)

This may also explain the stronger impact of sucralose on intrinsic fluorescence. Complementary approaches such as isothermal titration calorimetry (ITC) would therefore be valuable to further measure sucrose and sucralose binding and determine their thermodynamic parameters independently of spectroscopic changes.

Concentration-response relationships for the tryptophan intrinsic fluorescence of SUMO-hTAS1R2-VFT were determined for 4 sweet-tasting compounds (sucralose, neotame, Ace-K and sucrose) (Fig. 7). All of these compounds increased the intrinsic fluorescence intensity of tryptophan, which was saturable for all compounds except sucrose, indicating the presence of conformational changes in SUMO-hTAS1R2-VFT. The addition of neotame (+ 5.9%), sucralose (+ 12.4%), Ace-K (+ 12.3%), and sucrose (+ 16.8%) increased the maximal fluorescence activity of SUMO-hTAS1R2-VFT. In addition, the K_d values of SUMO-hTAS1R2-VFT in the presence of these different sweet-tasting compounds were calculated and compared with those from previous research (Table 2). Neotame exhibited the highest affinity (K_d = 2.05 ± 0.42 µM) for SUMO-hTAS1R2-VFT, followed by Ace-K (K_d = 116 ± 15 µM), sucralose (K_d = 282 ± 44 µM), and sucrose (K_d > 100 mM). Our results were consistent with those of previous work on mouse and human TAS1R-VFTs and physiological data, which revealed that sugars (sucrose) had affinity in the millimolar range and K_d values in the micromolar range for intense sweeteners (sucralose, neotame, and Ace-K) [12,15]. However, the K_d values obtained for SUMO-hTAS1R2-VFT differed from those reported for hTAS1R2-VFT and full-length hTAS1R2, particularly for sucralose and Ace-K. The SUMO fusion tag may partially hinder access to the binding site or alter ligand-induced conformational changes within TAS1R2-VFT, affecting apparent affinity. In addition, comparisons with the full-length receptor should be made cautiously, as these measurements involved a different expression system and a protein containing 7TM, which may modulate ligand binding through structural or allosteric effects. Therefore, while these comparisons supported consistent ligand selectivity, absolute K_d values were not directly comparable across systems probably due to differences in protein constructs, expression systems, and experimental conditions, although relative affinity trends remain informative. Consistent with these hypotheses, the K_d values obtained here were generally higher (ranging from approximatively 1 to 2 orders of magnitude depending on the ligand) than those reported for hTAS1R2-VFT [15], but remained comparable to those measured for the full-length hTAS1R2 subunit for neotame and Ace-K [17]. Interestingly, the K_d value of neotame, the most potent sweetener tested, was the one most closely aligned with the EC_{50} values measured for hTAS1R2/hTAS1R3 in cellular assays [7,17]. K_d and EC_{50} values characterize different parameters (binding affinity versus functional response) and are not directly comparable. In this study, the differences between them could be explained by heteromerization of the subunits, inter-subunit allosteric effects, or coupling of the TAS1R2/TAS1R3 receptor to the intracellular G-protein. assay [37].

4. Discussion

The TAS1R2 and TAS1R3 subunits, which belong to the C-GPCR class, assemble to form a single sweet taste receptor [38] capable of detecting various sweet-tasting chemical compounds (natural sugars, natural and artificial sweeteners, or sweet-tasting proteins) [2,4,12]. Here, we report the successful production of soluble, folded, and functional hTAS1R2-VFT in *E. coli* using a SUMO protein fusion. CD spectroscopy analysis revealed that SUMO-hTAS1R2-VFT was properly folded with secondary structures similar to those of mouse and human TAS1R-VFTs [12,15,16]. Gel filtration and SEC-MAL analysis revealed that SUMO-hTAS1R2-VFT behaved as a monomer, as previously reported for cat TAS1R1-VFT and human TAS1R1-VFT [15,32]. These results indicated that SUMO-hTAS1R2-VFT is stable in a monomeric form, in contrast to previous studies reporting a dimeric configuration of mouse and human TAS1R2-VFT, as well as human TAS1R3-VFT, as determined by gel filtration of proteins refolded from IBs [16,27].

Intrinsic tryptophan fluorescence analysis revealed that purified soluble SUMO-hTAS1R2-VFT was functional and capable of binding different sweet stimuli. It would be interesting to further investigate binding properties using ITC, particularly if SUMO-hTAS1R2-VFT production yields could be increased, to obtain a direct and quantitative assessment of the thermodynamics of ligand binding and stoichiometry. Dissociation constants were determined for 1 natural sugar (sucrose) and 3 sweeteners (sucralose, neotame, and Ace-K), which are known to interact with the VFT domain of TAS1R2 [12–17]. Sucrose bound SUMO-hTAS1R2-VFT with a K_d value in the millimolar range, in accordance with previous results [12,15,16,28]. The 3 intense sweeteners displayed higher and distinct affinities (K_d values in the micromolar range), in agreement with their relative sweetness potencies [39]. Interestingly, the measured K_d values were higher for neotame, Ace-K, and sucrose than those previously reported for hTAS1R2-VFT and were similar to those obtained for the full-length hTAS1R2 subunit, indicating ligand-dependent differences of up to approximatively 1 to 2 orders of magnitude. For sucralose, the dissociation constant was higher than those reported for both hTAS1R2-VFT and hTAS1R2 [15,17]. Differences in K_d values between the VFT domain of TAS1R2 and the entire TAS1R2 subunit could be explained by the presence of the 7TM domain [15]. In a previous study, slightly lower K_d values for mTAS1R2-VFT were observed than predicted values deduced from behavioral studies

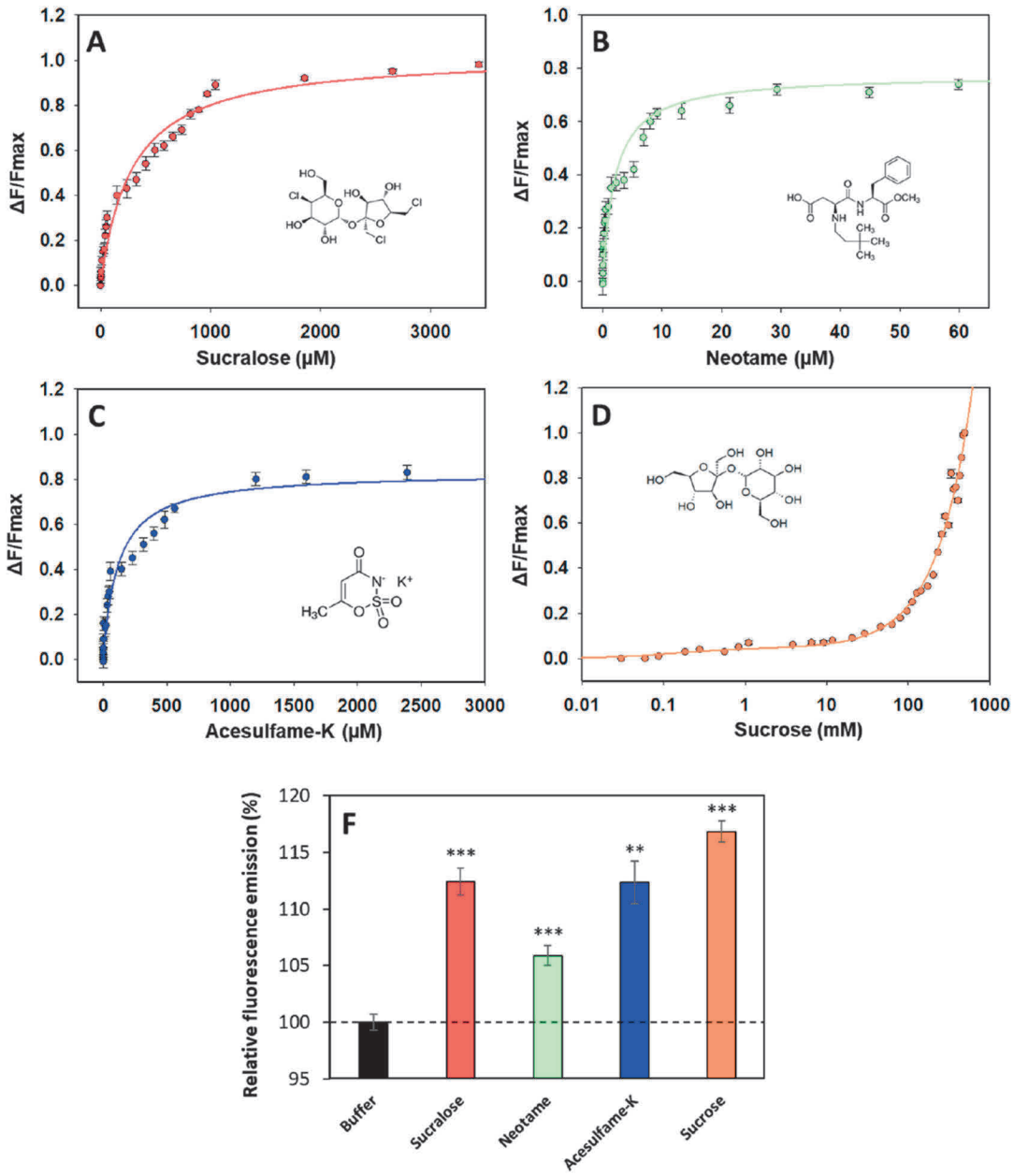

Fig. 7. Intrinsic tryptophan fluorescence of SUMO-hTAS1R2-VFT as a function of ligand concentration (A-D) for sucralose (red) (A), neotame (green) (B), acesulfame-K (blue) (C), or sucrose (orange) (D) and normalized maximal fluorescence intensity of SUMO-hTAS1R2-VFT after titration of buffer or ligand (F) (237 μM sucralose, 2.27 μM neotame, 144 μM acesulfame-K, or 222 mM sucrose). (A-D) The circles represent the experimental data, while the solid lines represent the computed binding curves; excitation and emission wavelengths were 295 and 350 nm, respectively; SUMO-hTAS1R2-VFT concentration was 0.10 mg/mL. Data points corresponded to mean ± SEM of more than 10 independent replicates of at least 6 independently soluble protein samples. Data were fitted with sigmoid dose-response curves using SigmaPlot 12.5 software. The chemical structure of each compound is shown. (F) *$p < 0.05$, **$p < 0.01$, ***$p < 0.001$, calculated using ANOVA followed by Dunnett's test for multiple comparison analysis (with reference to buffer). (For interpretation of the references to color in this figure legend, the reader is referred to the Web version of this article.)

carried out in rodents or receptor functional assays [12]. In addition, discrepancies in binding affinities may partly arise from the distinct expression systems used. Although K_d values obtained across different constructs and experimental systems were not strictly comparable in quantitative terms, and should therefore be interpreted with caution, they nevertheless allowed reliable comparison of relative affinity trends. We cannot rule out the possibility that SUMO influences the binding properties of hTAS1R2-VFT. The impact of interactions between the 2 subunits could also explain these binding differences. The 3D structure of the hTAS1R3/hTAS1R3 heterodimeric receptor has revealed inter-domain interactions between the 2 subunits [24–26], which could modulate the binding properties of hTAS1R2-VFT. Comparing the ligand affinities of the hTAS1R2-VFT/hTAS1R3-VFT heterodimer with that of the monomeric hTAS1R2-VFT should further elucidate this process. In our study, the isolated VFT domain was produced in *E. coli*, whereas the full-length hTAS1R2 subunit was expressed in an inducible HEK293S mammalian cell line [17]. Bacterial expression enables efficient and scalable production of soluble protein domains, making it particularly well suited for biochemical and ligand-binding analyses. However, it lacks the eukaryotic folding machinery and post-translational processing pathways that may contribute to optimal GPCR folding and domain coupling. In contrast, mammalian expression systems provide a more

Table 2
K_d values of SUMO-hTAS1R2-VFT (mean ± SEM of more than 10 independent replicates of at least 6 independently soluble protein samples) measured by intrinsic fluorescence for sucralose, neotame, acesulfame-K, and sucrose compared with the K_d values of hTAS1R2-VFT or hTAS1R2 and EC_{50} values determined by cellular assays.

Sweetener	SUMO-hTAS1R2-VFT (K_d)	hTAS1R2-VFT (K_d)	hTAS1R2[d] (K_d)	EC_{50} (hTAS1R2/hTAS1R3)
Sucralose	282 ± 44 μM	7.0 ± 1.3 μM[a]	29 ± 8 μM[b]	78 ± 11 μM[c]
Neotame	2.05 ± 0.42 μM	0.09 ± 0.02 μM[a]	2.78 ± 0.69 μM[b]	2.26 ± 0.23 μM[c]
Acesulfame-K	116 ± 15 μM	0.9 ± 0.2 μM[a]	164 ± 53 μM[b]	213 ± 59 μM[b]
Sucrose	>100 mM	4.2 ± 0.9 mM[a]	-	116 ± 40 mM[c]

[a] [15].
[b] [17].
[c] [7].
[d] Data from hTAS1R2 subunit overexpressed in absence of hTAS1R3 using an inducible HEK293S cell line.

native-like cellular environment, potentially improving folding fidelity, interdomain communication and structural stability, although they are generally less suited to large-scale production [27].

The presence of the SUMO domain could also modulate the interactions between each ligand and hTAS1R2-VTF, resulting in apparently lower affinities. One solution would involve removing the SUMO domain using a cleavage enzyme to obtain a soluble and functional hTAS1R2-VFT protein, as previously described [27]. However, cleavage introduces an additional processing step that may reduce protein yield and potentially compromise protein stability or functionality. Indeed, in this previous study [27], K_d values determined by CD spectroscopy were markedly higher than those measured for hTAS1R2-VFT in the presence of Ace-K, aspartame, neotame, saccharin, or sucralose [15], and higher than EC_{50} values measured for the hTAS1R2/hTAS1R3 receptor stimulated by neotame and saccharin [7,40]. Although K_d and EC_{50} values described distinct parameters (binding affinity versus functional response) and were not directly comparable, lower EC_{50} values in cellular assays are commonly explained by signal amplification and cooperative receptor activation [37]. As a next step, it would be interesting to cleave the SUMO domain and determine whether our protein of interest, hTAS1R2-VFT, remains soluble and functional. Finally, our intrinsic fluorescence data were largely consistent with the cell-based assay data obtained using the full-length hTAS1R2/hTAS1R3 receptor, except for sucralose, whose K_d value (282 ± 44 μM) was higher than the EC_{50} value (78 ± 11 μM) [17].

5. Conclusion

In this study, we established a novel and efficient strategy for producing soluble and functional hTAS1R2-VFT in *E. coli* using a SUMO fusion approach, eliminating the need for refolding from IBs. The purified protein was correctly folded, predominantly monomeric, and capable of binding a range of sweet-tasting compounds. Quantitative binding analyses revealed physiologically relevant affinities, with micromolar K_d values for high-intensity sweeteners and millimolar affinity for sucrose, consistent with their relative sweetness and EC_{50} values. Notably, the measured affinities were comparable to those reported for the full-length TAS1R2 receptor, supporting the functional relevance of the recombinant domain. Although further optimization could increase yields to levels comparable to those obtained with IB-based approaches [16,29] and clarify the influence of the SUMO tag, this approach provides a reproducible, and scalable platform for biophysical studies. Combined with complementary studies on the full-length receptor expressed in mammalian cells, this approach will be useful for studying ligand-binding interactions and complementary biophysical analysis. Compared with eukaryotic expression systems, it also offers an interesting and economical alternative due to its ease of implementation for screening sweeteners.

Funding sources

This research did not receive any specific grant from funding agencies in the public, commercial, or not-for-profit sectors.

CRediT authorship contribution statement

Christine Belloir: Conceptualization, Formal analysis, Funding acquisition, Investigation, Methodology, Project administration, Resources, Supervision, Validation, Visualization, Writing – review & editing. **Adeline Karolkowski:** Formal analysis, Visualization, Writing – original draft, Writing – review & editing. **Lucie Moitrier:** Investigation. **Loïc Briand:** Conceptualization, Funding acquisition, Project administration, Writing – review & editing.

Declaration of competing interest

The authors declare that they have no known competing financial interests or personal relationships that could have appeared to influence the work reported in this paper.

Appendix A. Supplementary data

Supplementary data to this article can be found online at https://doi.org/10.1016/j.pep.2026.106936.

Data availability

Data will be made available on request.

References

[1] L. Briand, C. Salles, Taste perception and integration, in: P. Etiévant, E. Guichard, C. Salles, A. Voilley (Eds.), Flavor from Food to Behaviors, Wellbeing and Health, Elsevier Ltd., Duxford, UK, 2016, pp. 101–119, https://doi.org/10.1016/B978-0-08-100295-7.00004-9.
[2] C. Belloir, F. Neiers, L. Briand, Sweeteners and sweetness enhancers, Curr. Opin. Clin. Nutr. Metab. Care 20 (2017) 279, https://doi.org/10.1097/MCO.0000000000000377.
[3] J.-P. An, Y. Wang, S.D. Munger, X. Tang, A review on natural sweeteners, sweet taste modulators and bitter masking compounds: structure-activity strategies for the discovery of novel taste molecules, Crit. Rev. Food Sci. Nutr. 65 (2025) 2076–2099, https://doi.org/10.1080/10408398.2024.2326012.
[4] X. Li, L. Staszewski, H. Xu, K. Durick, M. Zoller, E. Adler, Human receptors for sweet and umami taste, Proc. Natl. Acad. Sci. USA 99 (2002) 4692–4696, https://doi.org/10.1073/pnas.072090199.
[5] G. Nelson, M.A. Hoon, J. Chandrashekar, Y. Zhang, N.J.P. Ryba, C.S. Zuker, Mammalian sweet taste receptors, Cell 106 (2001) 381–390, https://doi.org/10.1016/S0092-8674(01)00451-2.
[6] A. Laffitte, F. Neiers, L. Briand, Characterization of taste compounds: chemical structures and sensory properties, in: Flavour, John Wiley & Sons, Ltd, 2016, pp. 154–191, https://doi.org/10.1002/9781118929384.ch7.
[7] C. Belloir, M. Jeannin, A. Karolkowski, C. Scott, L. Briand, A receptor-based assay to study the sweet and bitter tastes of sweeteners and binary sweet blends: the SWEET project, Chem. Senses 49 (2024) bjae041, https://doi.org/10.1093/chemse/bjae041.
[8] Y. Choi, J.A. Manthey, T.H. Park, Y.K. Cha, Y. Kim, Y. Kim, Correlation between in vitro binding activity of sweeteners to cloned human sweet taste receptor and sensory evaluation, Food Sci. Biotechnol. 30 (2021) 675–682, https://doi.org/10.1007/s10068-021-00905-z.

[9] G. Servant, C. Tachdjian, X. Li, D.S. Karanewsky, The sweet taste of true synergy: positive allosteric modulation of the human sweet taste receptor, TIPS (Trends Pharmacol. Sci.) 32 (2011) 631–636, https://doi.org/10.1016/j.tips.2011.06.007.
[10] M. Cui, P. Jiang, E. Maillet, M. Max, R.F. Margolskee, R. Osman, The heterodimeric sweet taste receptor has multiple potential ligand binding sites, Curr. Pharm. Des. 12 (2006) 4591–4600, https://doi.org/10.2174/138161206779010350.
[11] H. Xu, L. Staszewski, H. Tang, E. Adler, M. Zoller, X. Li, Different functional roles of T1R subunits in the heteromeric taste receptors, Proc. Natl. Acad. Sci. USA 101 (2004) 14258–14263, https://doi.org/10.1073/pnas.0404384101.
[12] Y. Nie, S. Vigues, J.R. Hobbs, G.L. Conn, S.D. Munger, Distinct contributions of T1R2 and T1R3 taste receptor subunits to the detection of sweet stimuli, Curr. Biol. 15 (2005) 1948–1952, https://doi.org/10.1016/j.cub.2005.09.037.
[13] F. Zhang, B. Klebansky, R.M. Fine, H. Liu, H. Xu, G. Servant, M. Zoller, C. Tachdjian, X. Li, Molecular mechanism of the sweet taste enhancers, Proc. Natl. Acad. Sci. USA 107 (2010) 4752–4757, https://doi.org/10.1073/pnas.0911660107.
[14] K. Masuda, A. Koizumi, K. Nakajima, T. Tanaka, K. Abe, T. Misaka, M. Ishiguro, Characterization of the modes of binding between human sweet taste receptor and low-molecular-weight sweet compounds, PLoS One 7 (2012) e35380, https://doi.org/10.1371/journal.pone.0035380.
[15] A. Laffitte, C. Belloir, F. Neiers, L. Briand, Functional characterization of the Venus flytrap domain of the human TAS1R2 sweet taste receptor, Int. J. Mol. Sci. 23 (2022) 9216, https://doi.org/10.3390/ijms23169216.
[16] E. Maîtrepierre, M. Sigoillot, L.L. Pessot, L. Briand, Recombinant expression, *in vitro* refolding, and biophysical characterization of the N-terminal domain of T1R3 taste receptor, Protein Expr. Purif. 83 (2012) 75–83, https://doi.org/10.1016/j.pep.2012.03.006.
[17] C. Belloir, M. Brulé, L. Tornier, F. Neiers, L. Briand, Biophysical and functional characterization of the human TAS1R2 sweet taste receptor overexpressed in a HEK293S inducible cell line, Sci. Rep. 11 (2021) 22238, https://doi.org/10.1038/s41598-021-01731-3.
[18] N. Dubovski, Y. Ben Shoshan-Galeczki, E. Malach, M.Y. Niv, Taste and chirality: l-glucose sweetness is mediated by TAS1R2/TAS2R3 receptor, Food Chem. 373 (2022) 131393, https://doi.org/10.1016/j.foodchem.2021.131393.
[19] C. Cai, H. Jiang, L. Li, T. Liu, X. Song, B. Liu, Characterization of the sweet taste receptor Tas1r2 from an old world monkey species rhesus monkey and species-dependent activation of the monomeric receptor by an intense sweetener perillartine, PLoS One 11 (2016) e0160079, https://doi.org/10.1371/journal.pone.0160079.
[20] P. Jiang, M. Cui, B. Zhao, L.A. Snyder, L.M.J. Benard, R. Osman, M. Max, R. F. Margolskee, Identification of the cyclamate interaction site within the transmembrane domain of the human sweet taste receptor subunit T1R3, J. Biol. Chem. 280 (2005) 34296–34305, https://doi.org/10.1074/jbc.M505255200.
[21] M. Winnig, B. Bufe, N.A. Kratochwil, J.P. Slack, W. Meyerhof, The binding site for neohesperidin dihydrochalcone at the human sweet taste receptor, BMC Struct. Biol. 7 (2007) 66, https://doi.org/10.1186/1472-6807-7-66.
[22] P. Jiang, Q. Ji, Z. Liu, L.A. Snyder, L.M.J. Benard, R.F. Margolskee, M. Max, The cysteine-rich region of T1R3 determines responses to intensely sweet proteins, J. Biol. Chem. 279 (2004) 45068–45075, https://doi.org/10.1074/jbc.M406779200.
[23] F.M. Assadi-Porter, E.L. Maillet, J.T. Radek, J. Quijada, J.L. Markley, M. Max, Key amino acid residues involved in multi-point binding interactions between brazzein, a sweet protein, and the T1R2–T1R3 human sweet receptor, J. Mol. Biol. 398 (2010) 584–599, https://doi.org/10.1016/j.jmb.2010.03.017.
[24] Z. Shi, W. Xu, L. Wu, X. Yue, S. Liu, W. Ding, J. Zhang, B. Meng, L. Zhao, X. Liu, J. Liu, Z.-J. Liu, T. Hua, Structural and functional characterization of human sweet taste receptor, Nature 645 (2025) 801–808, https://doi.org/10.1038/s41586-025-09302-6.
[25] H. Wang, X. Chen, Y. Dai, S. Pidathala, Y. Niu, C. Zhao, S. Li, L. Wang, C.-H. Lee, Structure and activation mechanism of human sweet taste receptor, Cell Res. (2025) 1–4, https://doi.org/10.1038/s41422-025-01156-x.
[26] Z. Juen, Z. Lu, R. Yu, A.N. Chang, B. Wang, A.W.P. Fitzpatrick, C.S. Zuker, The structure of human sweetness, Cell 188 (2025) 4141–4153.e18, https://doi.org/10.1016/j.cell.2025.04.021.
[27] F.M. Assadi-Porter, J. Radek, H. Rao, M. Tonelli, Multimodal ligand binding studies of human and mouse G-Coupled taste receptors to correlate their species-specific sweetness tasting properties, Molecules 23 (2018) 2531, https://doi.org/10.3390/molecules23102531.
[28] Y. Nie, J.R. Hobbs, S. Vigues, W.J. Olson, G.L. Conn, S.D. Munger, Expression and purification of functional ligand–binding domains of T1R3 taste receptors, Chem. Senses 31 (2006) 505–513, https://doi.org/10.1093/chemse/bjj053.
[29] E. Maîtrepierre, M. Sigoillot, L. Le Pessot, L. Briand, An efficient Escherichia coli expression system for the production of a functional N-terminal domain of the T1R3 taste receptor, Bioengineered 4 (2013) 25–29, https://doi.org/10.4161/bioe.21877.
[30] S.-B. Jin, H.-A. Kim, J.-A. Shin, N.-H. Jung, S.-Y. Park, S. Hong, K.-H. Kong, Recombinant expression and tryptophan-assisted analysis of human sweet taste receptor T1R3's extracellular domain in sweetener interaction studies, Prep. Biochem. 54 (2024) 1196–1203, https://doi.org/10.1080/10826068.2024.2336985.
[31] C. Belloir, L. Moitrier, A. Karolkowski, N. Poirier, F. Neiers, L. Briand, Inosine-5′-monophosphate interacts with the TAS1R3 subunit to enhance sweet taste detection, Food Chem.: Mol. Sci. 10 (2025) 100246, https://doi.org/10.1016/j.fochms.2025.100246.
[32] C. Belloir, J. Savistchenko, F. Neiers, A.J. Taylor, S. McGrane, L. Briand, Biophysical and functional characterization of the N-terminal domain of the cat T1R1 umami taste receptor expressed in Escherichia coli, PLoS One 12 (2017) e0187051, https://doi.org/10.1371/journal.pone.0187051.
[33] H. Yamaguchi, M. Miyazaki, Refolding techniques for recovering biologically active recombinant proteins from inclusion bodies, Biomolecules 4 (2014) 235–251, https://doi.org/10.3390/biom4010235.
[34] F. Guerrero, A. Ciragan, H. Iwaï, Tandem SUMO fusion vectors for improving soluble protein expression and purification, Protein Expr. Purif. 116 (2015) 42–49, https://doi.org/10.1016/j.pep.2015.08.019.
[35] H. Wang, Y. Xiao, L. Fu, H. Zhao, Y. Zhang, X. Wan, Y. Qin, Y. Huang, H. Gao, X. Li, High-level expression and purification of soluble recombinant FGF21 protein by SUMO fusion in Escherichia coli, BMC Biotechnol. 10 (2010) 14, https://doi.org/10.1186/1472-6750-10-14.
[36] A. Micsonai, F. Wien, N. Murvai, M.P. Nyiri, B. Balatoni, Y.-H. Lee, T. Molnár, Y. Goto, F. Jamme, J. Kardos, BeStSel: analysis site for protein CD spectra—2025 update, Nucleic Acids Res. 53 (2025) W73–W83, https://doi.org/10.1093/nar/gkaf378.
[37] P. Buchwald, Quantification of signal amplification for receptors: the Kd/EC50 ratio of full agonists as a gain parameter, Front. Pharmacol. 16 (2025), https://doi.org/10.3389/fphar.2025.1541872.
[38] M. Behrens, L. Briand, C.A. de March, H. Matsunami, A. Yamashita, W. Meyerhof, S. Weyand, Structure–function relationships of olfactory and taste receptors, Chem. Senses 43 (2018) 81–87, https://doi.org/10.1093/chemse/bjx083.
[39] S.S. Schiffman, C.A. Gatlin, Sweeteners: state of knowledge review, Neurosci. Biobehav. Rev. 17 (1993) 313–345, https://doi.org/10.1016/S0149-7634(05)80015-6.
[40] C. Belloir, M. Jeannin, A. Karolkowski, L. Briand, *TAS1R2/TAS1R3* single-nucleotide polymorphisms affect sweet taste receptor activation by sweeteners: the SWEET project, Nutrients 17 (2025) 949, https://doi.org/10.3390/nu17060949.